Isolated Pd Sites as Selective Catalysts for Electrochemical and Direct Hydrogen Peroxide Synthesis

Marc Ledendecker[a,b], Enrico Pizzutilo[a], Grazia Malta[c], Guilherme V. Fortunato[a,d], Karl J. J. Mayrhofer[a,e,f], Graham J. Hutchings[c] and Simon J. Freakley[g]*

[a] Department of Interface Chemistry and Surface Engineering, Max-Planck-Institut für Eisenforschung GmbH, Max-Planck-Strasse 1, 40237 Düsseldorf, Germany.

[b] Department of Technical Chemistry, Technical University Darmstadt, Alarich-Weiss Straße 8, 64287 Darmstadt, Germany

[c] Cardiff Catalysis Institute, School of Chemistry, Cardiff University, Main Building, Park Place, Cardiff, CF10 3AT, UK.

[d] Institute of Chemistry, Universidade Federal de Mato Grosso do Sul; Av. Senador Filinto Muller, 1555; Campo Grande, MS 79074-460, Brazil.

[e] Helmholtz-Institute Erlangen-Nürnberg for Renewable Energy (IEK-11), Forschungszentrum Jülich, Egerlandstr. 3, 91058 Erlangen, Germany.

[f] Department of Chemical and Biological Engineering, Friedrich-Alexander-Universität Erlangen-Nürnberg, Egerlandstr. 3, 91058 Erlangen, Germany.

[g] Department of Chemistry, University of Bath, Claverton Down, Bath, BA2 7AY, UK.

*s.freakley@bath.ac.uk

Abstract

Palladium nanoparticles have been studied extensively as catalysts for the direct synthesis of hydrogen peroxide, where selectivity remains a key challenge. Alloying Pd with other metals and the use of acid and halide promoters are commonly used to increase H_2O_2 selectivity, however; the sites that can selectively produce H_2O_2 have not been identified and the role of these additives remains unclear. Here, we report the synthesis of atomically dispersed Pd/C as a model catalyst for H_2O_2 production without the presence of extended Pd surfaces. We show that these isolated cationic Pd sites can form H_2O_2 with significantly higher selectivity than metallic Pd nanoparticles in both the reaction of H_2 and O_2 and the electrochemical oxygen reduction reaction. These results demonstrate that catalysts containing high populations of isolated Pd sites are selective catalysts for this two-electron reduction reaction and that the performance of materials in the direct synthesis reaction and electrocatalytic oxygen reduction reaction have many similarities.

Keywords – Catalysis, Hydrogen Peroxide, Palladium, Electrocatalysis

TOC

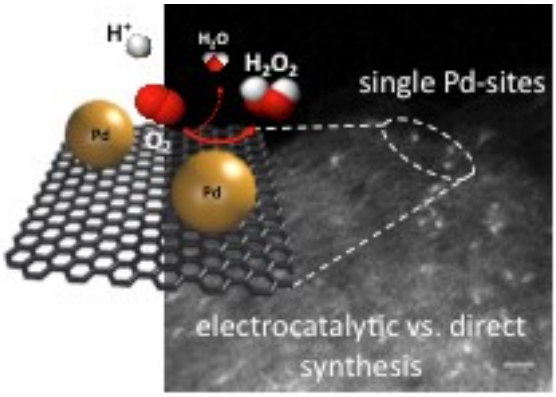

Introduction

Hydrogen peroxide (H_2O_2) is an increasingly important commodity chemical due to its high oxidation potential and low environmental impact due to water being the only by-product of its many applications.[1] H_2O_2 is currently used extensively in the pulp and paper industry and increasingly in selective oxidation processes at large scale; such as the hydrogen peroxide propene oxide (HPPO) process.[2] In addition, H_2O_2 is considered a key component in future water purification technology in remote areas.[3] Currently the vast majority of H_2O_2 is produced through the indirect anthraquinone process via the sequential reduction and oxidation of a substituted anthraquinone in an organic working solution.[4] While highly optimized and able to produce large quantities of concentrated H_2O_2, new approaches are being continually sought to allow decentralized continuous production of H_2O_2 at the point of use without the need for storage and transport.[5, 6]

The selective catalytic production of H_2O_2 from molecular hydrogen (H_2) and oxygen (O_2) has been a target for Pd heterogeneous catalysts since the first patents appeared in 1914.[7] Numerous Pd nanoparticle based catalysts have been extensively studied as promising candidates for this challenging hydrogenation, although systems with satisfactorily high selectivity and rate are limited. The problems of over hydrogenation and decomposition of H_2O_2 to produce H_2O limits the application of monometallic Pd catalysts without the addition of additives to the reaction or alloying with secondary metals to form bimetallic catalysts. These systems have recently been extensively reviewed by numerous groups highlighting the potential of this process.[8-14] Typically, acid and halide additives are used to stabilize the synthesized H_2O_2 and increase selectivity based on H_2. It is postulated that halide additives can selectivity block high activity Pd sites on nanoparticles reducing over hydrogenation rates.[15-17] Alternatively, bimetallic particles with noble metals such as Au[18-20] and base metal such as Sn[21], Ni[22] and Zn[23, 24] have been shown to be able to produce H_2O_2 with high efficiency and in some cases with H_2 selectivity over 95% in the absence of acid and halides, demonstrating that the sites for H_2O_2 synthesis and H_2O_2 degradation are different and can be isolated.[20, 21]

Recently, based on a comprehensive kinetic analysis to determine the effects of H_2 and O_2 partial pressure, temperature and pH (including the use of protic and aprotic solvents) it was proposed that the mechanism of H_2O_2 formation on Pd involves sequential electron-proton transfer to surface bound O_2 and OOH species rather than a purely Langmuir type surface model.[25] This mechanism implies that two half reactions are occurring at the metal nanoparticle; hydrogen oxidation to protons to supply electrons for the oxygen reduction by proton-coupled electron transfer, rationalizing the observed dependence on pH and the need

for protic solvents. This also dictates that when using a non-conducting catalyst support, such as TiO_2 and SiO_2, both reactions must occur simultaneously on the same nanoparticle. These two half reactions, akin to a fuel cell, rely on the chemical potential of H_2 as the driving force for the reaction and is analogous to applying an electrical potential to drive the oxygen reduction reaction electrochemically. This suggests that materials that are selective towards the two-electron oxygen reduction in the reaction of H_2 and O_2 will be selective in electrochemical ORR and HOR if they are conductive and vice versa, selective ORR catalysts should perform well in the direct synthesis reaction if they are able to activate H_2.

While Pd and Pt typically catalyze the 4-electron reduction of O_2 to H_2O, a number of materials have been identified as potential catalysts for the 2-electron reduction of O_2 to H_2O_2. with an overview given recently by Stephens and coworkers.[26-29] Bare carbon-based materials have been shown to achieve high selectivity in the half-cell ORR to form H_2O_2, however, the reaction rates for the HOR are usually low, severely limiting activity for the direct synthesis reaction in the absence of precious metals.[30] In contrast, extended Pd/Pt surfaces are highly active towards the HOR and the reduction of O_2 often resulting in O-O bond rupture and therefore low selectivity.[31]

One apporoach to achieve high selectivity is surface blocking with amorphous carbon layers allowing diffusion of reactants to the surface and promoting end-on rather than side-on binding of O_2 – suppressing H_2O formation and reaching H_2O_2 selectivity of 30% at 0.3 V.[32] Numerous studies have focused on alloying two metals to achieve synergistic effects between metals that bind O_2 strongly such as Pt and Pd with a second metal that binds O_2 weakly such as Au and Hg.[33-35] These studies typically report improved selectivity towards H_2O_2 compared to the monometallic Pd or Pt catalysts through both site isolation and electronic effects. A key example of this approach is a PdHg/C catalyst, which can achieve a selectivity of around 90% towards H_2O_2 at 0.3 - 0.5 V and has been shown to consist of nanoparticles containing a metallic Pd core and a PdHg alloy outer shell.[36,37] In addition to challenges around mercury toxicity, to the best of our knowledge, no examples of Hg based hydrogenation catalysts have been reported suggesting that the direct production of H_2O_2 on bare Hg will be limited as the activity for the HOR will be low. As overpotentials over 1 V at 25 °C were reported to catalyse the hydrogen evolution reaction, similar overpotentials for the HOR are expected. At the limits of site isolation, isolated Pt species have recently been stabilized on TiC[38] and TiN[39] supports with potential dependent H_2O_2 selectivity between 60-80%. High sulfur containing (17 wt%) carbonaceous materials have been shown to support high dispersion of Pt and demonstrate high selectivity (95% at 0.71V onset potential) towards H_2O_2 in the ORR in addition to Co-

porphyrin containing catalysts which were able to achieve 90 % selectivity (at -0.1 V) with an onset potential of approx. 0.5 V in a RRDE setup.[40,41]

In this study, we report the synthesis of an atomically dispersed carbon supported Pd catalyst and show that this material is highly selective in both, the electrochemical ORR/HOR and the direct synthesis reaction to produce H_2O_2 from molecular H_2 and O_2. Through electrochemical half-cell testing, the HOR and ORR can be investigated independently and conclusions for the direct synthesis can be drawn. The material shows that continuous production of H_2O_2 is possible with high atom efficiency using precious metal catalysts without the need to design bimetallic alloys or selectively block nanoparticle surface sites.

Results and Discussion

Studies by Schriffin and Jirkovský have shown that low levels of Pd in Au rich AuPd bimetallic nanoparticles could act as reactive "hot-spots" with increased 2-electron ORR selectivity, in agreement with our own observations that as Pd is selectively leached from AuPd nanoparticles 2-electron ORR selectivity is increased.[33,42,43] This led us, in combination with the recent kinetic studies on direct H_2O_2 synthesis from H_2 and O_2, to hypothesize that isolated Pd sites supported on conductive materials could act as selective catalysts for both the electrochemical ORR and the direct synthesis of H_2O_2 from H_2/O_2 mixtures via the type of coupled proton-electron recently proposed.[25] We recently reported the synthesis and characterization of an atomically dispersed 1% Au / C catalyst which was shown to be stable at high temperatures.[44] This catalyst was prepared by the deposition of Au onto activated carbon from an aqua regia solvent before drying at 140 °C. We extended this approach to the synthesis of 1% Pd/C using a $PdCl_2$ precursor and Norit ROX 0.8 carbon support by incipient wetness, the catalyst material was prepared on a 2 g scale.

Initial characterization of the catalyst material by X-ray photoemission spectroscopy (XPS) to confirm the presence and oxidation state of Pd are shown in Figure 1a. The spectra of the Pd 3d region shows the expected splitting and binding energy of oxidized Pd species (Pd (II) $3d_{5/2}$ - 337.4 eV) with no presence of secondary metallic Pd speciation (Pd $3d_{5/2}$ - 335.0 eV).[45] This is consistent with the highly oxidizing nature of the impregnation solvent followed by heat treatment under inert atmosphere and confirms the deposition of the Pd precursor onto the carbon surface. Table S1 reports the surface composition of the as-prepared catalyst and confirms a Pd loading of 0.16 at% corresponding to 1.3 wt%, in addition to significant Cl (6.7 wt%) and O content (8.1 wt%) on the carbon surface. Chlorine (1s) binding energies (Figure S1) are suggestive of the presence of both inorganic and organic Cl species on the catalyst

surface. However, organic Cl dominate the signal with binding energies of ~200 eV suggesting formation of C-Cl surface groups.

X-Ray diffraction (XRD) analysis of the freshly prepared 1% Pd/C to exclude the formation of crystalline PdO/Pd (Figure 1b) revealed the absence of the principle reflections of either nanocrystalline metallic Pd (111) at 45° (JCPDS no: 46-1043) or PdO (101) at 40° (JCPDS no: 41-1107) using a Co K_α radiation source, indicating either the metal crystallite size or metal loading of the catalyst is below the limits of detection. For comparison a 1% Pd/C prepared by sol immobilization containing metallic Pd nanoparticles with average size 4.3 ± 1.0 nm determined by TEM, (Figure S2) and denoted as (Pd_{np}/C) is also included in addition to the bare carbon support which both also show the absence of diffraction peaks.

We performed *in situ* XRD of the fresh catalyst material at increasing temperatures under an Ar atmosphere to determine if the possible high dispersion of Pd was susceptible to thermally induced sintering/decomposition. Figure 1c shows that the absence of diffraction patterns is maintained at 400 °C suggesting the possible high dispersion of Pd species remains strongly anchored to the support material. Transmission electron microscopy (TEM) imaging at low and medium magnifications (Figure 1d) of the fresh sample revealed the absence of Pd nanoparticles in the nanometer size range on the carbon support material consistent with the XRD observations. High-angle annular dark-field scanning transmission electron microscopy (HAADF-STEM) (Figure 1e) revealed the presence of a population of Pd species significantly smaller than 1 nm appearing in near atomic dispersion with the absence of any Pd nanoparticle structures. This suggests that the Pd/C catalyst material does not contain extended Pd surfaces or small metallic Pd nanoparticles which have been suggested to lead to low H_2O_2 selectivity in the direct synthesis or ORR reactions through promotion of over hydrogenation.

X-ray absorption spectroscopy of the highly dispersed catalyst (Figure 2a) at the Pd K-edge supported the observations of the XPS measurements that the Pd is in a cationic state (edge position – 24,354 eV) consistent with existing literature and clearly higher than the absorption edge of a metallic Pd foil (edge position – 24,350 eV) recorded during the same experiment. In addition, significantly different post edge structure were observed suggesting that the Pd is not present as metallic nanoparticles below the diffraction limit.[46] Extended X-ray Absorption Fine Structure non-phase corrected analysis (Figure 2b) further corroborates the absence of higher nuclearity Pd structures. In comparison to the metallic Pd foil, the synthesized catalyst shows no features in the Fourier transform consistent with recorded standards and literature examples of scattering intensity resulting from Pd-Pd scattering paths in metallic Pd structures.[46] When compared to other cationic Pd standards (Figure 2c,d), the recorded spectra of the catalyst

better match the reference $PdCl_2$ spectra suggesting that the shortest scattering event is not consistent with the Pd-Pd or Pd-O scattering of metallic Pd or PdO but a Pd-Cl scattering path (Pd-Cl coordination number – 3.99 ± 0.4, fitting parameters shown in Figure S3). Additional low energy XAS at the Cl K-edge shown in figure 2e revealed the presence of two distinct Cl features consistent with C-Cl and Pd-Cl chlorine environments in the catalyst material suggesting highly dispersed cationic Pd species with a Cl ligand environment (denoted at $PdCl_x$/C subsequently).[47,48] Comparing the EXAFS model of the first co-ordination shell of the $PdCl_2$ standard with our catalyst material reveals no significant shift in the position of the scattering event on forming the dried catalyst material. This indicates that there is limited additional scattering paths, such as Pd-O or Pd-N, between the Pd and catalyst surface in the catalyst material. These bond lengths would be considerably shorter than the Pd-Cl – for example Pd-O based on Pd acetate as a model of a Pd-O-C would be approximately 0.3 Å shorter than the observed intensity consistent with Pd-Cl.[49] As we see no change in Pd-Cl coordination or agglomerates in the STEM analysis, we suggest that $PdCl_4^{2-}$ is adsorbed to the carbon surface mainly through electrostatic interactions rather than ligand exchange with oxygen containg groups on the carbon surface. Another possibility is that chorine on the surface of the carbon as a result of the aqua regia treatment could be the anchor point between the carbon and Pd species – providing bridgning Cl spcies similar to the bulk structure of $PdCl_2$.

Recently it has been suggested that the mechanism of direct synthesis of H_2O_2 from H_2 and O_2 could follow an electrochemical type ORR mechanism initiated by the oxidation of H_2 into protons with coupled electron transfer to adsorbed O_2 or OOH species on the same particle.[25] In this case, good correlations should be able to be made through studying the electrochemical ORR and direct synthesis using the same materials. In our previous studies using AuPd nanoparticles with varying Au : Pd ratios, these correlations can be seen between catalyst activity and selectivity at certain electrochemical potentials – presumably these potentials correspond to the chemical potential of the heterogeneous reactor system at our chosen reaction conditions.[33, 35, 50, 51] Using the synthesized single site Pd catalyst, the activity in the direct synthesis reaction could be expected to be greatly reduced if adjacent Pd sites are required for H_2 activation. A study by Han *et al.* recently reported that in fact single Pd sites supported on hydroxyapatite ($CaPO_4$) showed limited activity for H_2O_2 synthesis and low nuclearity Pd clusters were required for H_2 activation,[52] although single site Pd supported on a carbon nitride material has been shown to be active for alkene/alkyene hydrogenation in liquid phase heterogeneous systems previously.[53] In contrast during electrochemical ORR in acidic media, the H^+/e^- couple is supplied to the catalyst surface without the requirement for H_2 activation removing the requirement for H_2 activation to produce H_2O_2.

To compare the surface structure and the potential dependent surface coverage of adsorbing species, cyclic voltammetry of the atomically dispersed 1% $PdCl_x$/C catalyst was investigated and compared to a 1% Pd/C catalyst prepared by our previously reported sol-immobilsation methods to generate metallic Pd nanoparticles with a 2-6 nm size distribution (Figure S2) (denoted as 1% Pd_{np}/C) (Figure 3a).[50 51] Inspection of the voltammograms between 0.1 and 1.6 V_{RHE} revealed markedly different redox characteristics, especially in the region of hydrogen underpotential deposition (H_{UPD}, $H^+ + e^- \rightarrow H_{upd}$) between $0.05 < E < 0.4$ V_{RHE}, adsorption of hydroxyl species (OH_{ad}, $H_2O \rightarrow OH_{ad} + H^+ + e^-$) above 0.65 V_{RHE} and the oxidation and reduction of Pd/PdO over 1.05 V_{RHE} and between $0.7 > E > 0.4$ V_{RHE}, respectively. The voltammogram of 1% Pd_{np}/ C was entirely consistent with the literature for supported Pd catalysts possessing the described redox features of potential-dependent adsorbing species and Pd-oxidation and reduction. The adsorption of hydrogen at H_{UPD} could drive the formation of Pd-hydrides in both the electrochemical and heterogeneous reactions, which has recently been observed spectroscopically during operando XAS measurements of Pd and AuPd catalysts during H_2O_2 synthesis.[54] It has been suggested that these hydride phases can contribute towards H_2O_2 degradation and it is known that extended Pd facets can facilitate O=O bond cleavage leading to eventual water formation.[55, 56] In contrast, the $PdCl_x$/C with atomic dispersion showed no redox features consistent with the bulk reduction of PdO on the cathodic sweep despite being previously exposed to potentials of 1.5 V_{RHE} during the anodic sweep confirming the significantly different nanostructure of this catalyst. In addition, no associated charge in the hydrogen underpotential deposition region was observed suggesting a general lack of H-underpotential adsorption sites. The electrochemical features were maintained after 1000 voltammetry cycles between 0.05 – 0.8 V_{RHE} supporting the high stability in the potential window encompassing ORR onset and the dispersed Pd-Cl species not only was resident to sintering but also to bulk oxidation and reduction (Figure S4).

The nature of electrocatalytic testing allows the same catalyst to be tested separately for both half reactions involved in the synthesis of H_2O_2 in heterogeneous systems, the $2e^-$ oxygen reduction and hydrogen oxidation reactions (ORR and HOR respectively). The bifunctionality of $PdCl_x$/C is demonstrated by the potentiodynamic oxidation of molecular hydrogen (HOR). Figure 3b shows the cyclic voltammetry at different rotation speeds in hydrogen saturated $HClO_4$ starting from 0.78 V_{RHE} sweeping negatively to the potential limit of -0.02 V_{RHE} at which point the sweep was reversed. Hydrogen gas was introduced continuously during the measurements in order to maintain a saturated solution. The low amount of supported catalyst leads to lower diffusion limiting currents than theoretically expected as the total number of Pd-atoms is too small to concede full overlap between adjacent diffusion zones. This behavior was

also observed during the diffusion limited ORR in acidic media for Pt-loadings below 0.042 mg_{Pt}/cm^2_{geo}.[57] We clearly demonstrate that $PdCl_x/C$ is active towards the electrocatalytic hydrogen oxidation and that both redox reactions – the HOR and ORR - can be evaluated separately with possibility to use these descriptors to predict direct H_2O_2 synthesis activity in heterogeneous systems.

Figure 3c displays a characteristic set of current-voltage polarization curves for the oxygen reduction reaction on $PdCl_x/C$, 1% Pd_{np}/C and the aqua regia treated bare carbon as reference in 0.1M $HClO_4$. For the standard nanoparticle containing 1% Pd_{np}/C, well defined diffusion limiting currents for the 4e- transfer reaction of O_2 to H_2O were observed from 0.35 to 0.7 V_{RHE}, followed by a mixed kinetic-diffusion controlled region between 0.8 and 1.0 V_{RHE}. The selectivity (Figure 3d) towards H_2O_2 measured by the ring current over the potential range from 1 to 0.1 V_{RHE} was below 5% across the whole potential range. The onset potential for oxygen reduction was significantly different (0.9 V_{RHE}) compared to $PdCl_x/C$ (0.6 V_{RHE}) showing that the nanostructure remains considerably different in the electrolyte solution. In contrast, the atomically dispersed $PdCl_x/C$ achieves selectivity to H_2O_2 above 90% with a mass normalized activity of 72.8 A g_{Pd}^{-1} which is among the best known oxygen to hydrogen peroxide reduction catalysts reported to date in acidic media without the need for alloying or surface blocking and also among the most selective catalysts.[27, 40] A comparison with the state of the art literature is included in figure S5. The aqua regia treated carbon as reference showed similar H_2O_2 selectivity over the tested potential range but significantly higher overpotentials and a low activity towards the 2-electron oxygen reduction reaction. The results show that isolated cationic $PdCl_x$ sites can make H_2O_2 selectively with little activity towards H_2O_2 degradation in the electrochemical ORR, showing distinct behavior compared to Pd nanoparticles which catalyze the 4-electron reduction with near complete selectivity. These results highlight the need to isolate Pd sites to produce selective catalysts for H_2O_2 synthesis.

Ex-situ pre- (beginning-of-life; BOL) and post-catalytic (end-of-life, EOL) Pd and Cl XPS measurements of the electrode containing the $PdCl_x/C$ catalyst after electrochemical cycling above and below the ORR onset confirm the retention of the of Cl speciation. Binding energies associated with inorganic and organic chlorine after cycling supports the high stability of these species (Figure 4a). Higher binding energy Cl speciation was present in the used sample associated with ClO_4^- retained on the catalyst surface from the electrolyte. No metallic Pd speciation were detected suggesting that the high surface energy single atoms are not being reduced in the course of the reaction. Additionally, electrolyte aliquots were taken during an extended degradation protocol consisting of 1000 cycles between 0.05 and 0.8 V (above and below the ORR onset) and analyzed via inductively coupled plasma mass spectrometry (ICP-

MS) as shown in Figure 4e. After 10 cycles, the catalyst stabilizes and only minimal Pd-loss was observed subsequently. After 1000 degradation cycles, over 83 at% of Pd was maintained in the catalyst and most Pd dissolves in the first 10 cycles until the surface stabilizes which is commonly observed for noble and non-noble electrocatalysts.

In the direct reaction between H_2 and O_2 to form H_2O_2, molecular H_2 must be cleaved - Pd surfaces or ensembles are capable of cleaving H_2 with high rates. Alone, however, they are likely to result in significant H_2O formation without the addition of a second metal or additives. Indeed, under our H_2O_2 direct synthesis conditions in the absence of acid and halide additives, the 1% Pd_{np}/C catalyst containing 2-5 nm Pd nanoparticles prepared by sol-immobilization showed high productivity rates for H_2O_2 synthesis and also high rates of H_2O_2 over-hydrogenation and degradation consistent with the reported ability of the Pd particles to catalyze O=O bond cleavage and water formation through over hydrogenation Table 1.[51]

Table 1 – Direct synthesis and H_2O_2 degradation productivity of catalysts containing metallic Pd nanoparticles and isolated $PdCl_x$ species.

Catalyst	**H_2O_2 Productivity[a] (mol / kg / h)**	**H_2O_2 Degradation Rate[b] (mol / kg / h)** (% H_2O_2 degraded during test)
Aqua regia treated carbon	0	45 (2%)
1% $PdCl_x$/C – aqua regia	30	52 (3%)
1% Pd_{np}/C – sol immobilization	120	360 (20%)

[a] 2 °C, 10 mg catalyst, 29 bar 5% H_2/CO_2, 11 bar 25% O_2/CO_2, 8.5 g solvent (5.6 g CH_3OH + 2.9 g H_2O) 1200 rpm, 30 mins.

[b] 2 °C, 10 mg catalyst, 29 bar 5% H_2/CO_2, 8.5 g solvent (5.6 g CH_3OH + 2.22 g H_2O + 0.68 g 50% H_2O_2 (10 mmol)) 1200 rpm, 30 mins.

Having shown that the $PdCl_x$/C catalyst is active for both, HOR and ORR electrochemically, the isolated Pd sites may favor only end-on binding of molecular oxygen, which has been postulated to be the reason for high selectivity in single site Pt catalysts for the 2 electron ORR leading to increased H_2O_2 formation.[31] Testing of the isolated site Pd catalyst in the autoclave system in the presence of H_2 and O_2 showed that the catalyst was capable of synthesizing H_2O_2 at appreciable rates (30 mol kg^{-1} h^{-1}) when compared to the nanoparticle catalyst. XAS and EXAFS analysis (Figure 4c,d) on the used $PdCl_x$/C catalyst showed minimal changes in the structure of the catalyst. The edge position remained constant indicating the palladium remained in a predominantly cationic state, suggesting that the H_2 + O_2 atmosphere did not reduce the Pd species or induce sintering to nanoparticles. A significant Pd-Cl scattering

intensity remained in the EXAFS analysis after the autoclave test (Pd-Cl coordination number 3.85 ± 0.5).

The activity of the catalyst material towards H_2O_2 degradation under a pressure of H_2 and in the presence of 4 wt % H_2O_2 was significantly lower than the nanoparticle containing catalyst and within the error of the activity of the aqua regia treated carbon alone. The testing of monometallic Pd catalysts is often carried out in the presence of strong mineral acids and halides to supress subsequent decomposition and hydrogenation of H_2O_2 so can not be used as a good comparison for intrinsic selectivity. A comparison of the activity of the atomically dispersed Pd/C with other catalysts able to achieve over 95% selectivity with respect to H_2 under the same reaction conditions is shown in table S2, demonstrating that the catalyst has comparative performance per mole of precious metal with other state of the art materials

These observations suggest that the same active species could be responsible for the activity and high selectivity in the electrochemical ORR and the direct synthesis of H_2O_2 from H_2 and O_2 – in this case, highly dispersed, strongly anchored $PdCl_x$ species. The lower observed activity per Pd atom in this system compared to other bimetallic formulations where extended Pd facets are broken, such as the well-studied AuPd systems, could arise from the lack of electronic promotion from alloying second metal components or the high stability of the ligand environment surrounding the isolated Pd centers. This provides a route for future catalyst design through ligand optimization of the isolated Pd centers for both electrochemical ORR and direct H_2O_2 synthesis.[58,59]

Considering the commonalities observed between the direct synthesis and electrochemical ORR reaction, it could be unlikely that a purely Langmuir type mechanism is in operation in both reactions as there is an absence of metallic Pd surfaces needed to support surface O_2/OH/OOH/H species. Additionally, there is no evidence of evolution of isolated $PdCl_x$ into nanoparticles which would lead to low selectivity as was observed using metallic Pd nanoparticle catalyst. The requirement to activate H_2 is removed in the electrochemical ORR as the H^+/e^- are supplied to the Pd bound oxygenate species by the electrolyte and electrode respectively. The observation of similar high selectivity in both systems could support the proposal of Flaherty *et. al* that the direct synthesis mechanism in heterogeneous catalyst systems does in fact proceed through an electrochemical type mechanism at the nanoparticle surface with electron conduction through the nanoparticle and protons shuttled through the protic solvent.[25] These observations are supported by the commonality observed between the performance of the same catalyst in the electrochemical and direct synthesis systems where catalyst evolution and subsequent reactions are minimal. Considering the proposal of Flaherty

et al. based on nanoparticle catalysts - electron transport is needed between the site of HOR and ORR, in a nanoparticle, the metallic conductivity could be responsible for this connection. In a system where only isolated Pd sites are observed, it is possible to consider two mechanisms; firstly, a mononuclear mechanism where O_2 and H_2 activation occur on the same Pd center – however, we see minimal change in the Pd-Cl coordination or oxidation state of the Pd. A second possibility is a cooperative mechanism where HOR and ORR occur on different Pd sites connected through the conductive support material – as we show that isolated Pd sites are active for both half reactions in isolation. This would be similar in nature to the two isolated half reactions occurring at different sites on the metal nanoparticle as proposed by Flaherty *et al*.[25] This mechanism – akin to fuel cell containing anodic and cathodic Pd sites connected electronically - could also explain the observation of limited activity for the previously reported highly dispersed Pd on non-conductive hydroxyapatite where small metallic Pd clusters were required for activity.[52]

Conclusions

Overall, our findings show that that isolated cationic Pd species are highly selective towards the 2-electron oxygen reduction reaction and show high mass activities. The synthesized single atom species are stable during electrochemical cycling, thermal treatment and under reaction condition in both electrochemical and heterogeneous H_2O_2 production. Our results suggest that the electrochemical half-cell reactions can be used as guideline for the development of selective H_2O_2 catalysts in heterogeneous catalysis.

Methods

Catalyst Preparation

1 wt% $PdCl_x/C$ – Activated carbon (Norit ROX 0.8) was initially ground to obtain a 100 - 140 mesh powder. The palladium precursor, $PdCl_2$ (Sigma Aldrich, 99%) was dissolved in 5.4 ml of aqua regia (3 parts by volume HCl [(Fisher, 32 wt.%)]: 1 part by volume HNO_3 [(Fisher, 70 wt. %)]). The palladium precursor solution was then added drop-wise with stirring to the activated carbon. Stirring was continued at ambient temperature until NO_x production had subsided. The product was then dried for 16 h at 140 ºC under an inert flow of nitrogen. An analogous method was used in the absence of Pd to generate the aqua regia carbon for control experiments.

1 wt% Pd_{np}/C – An aqueous solution of $PdCl_2$ (6 mg/ml) was prepared. Poly(vinyl alcohol) (PVA) (1 wt % aqueous solution, Aldrich, MW = 10 000, 80% hydrolyzed) and an aqueous solution of $NaBH_4$ (0.1 M) were also prepared. To 800 ml of water containing the appropriate amount of aqueous $PdCl_2$, the required amount of a PVA solution (1 wt %) was added (PVA/(Pd) (w/w) = 1.2); a freshly prepared solution of $NaBH_4$ (0.1 M, $NaBH_4$/(Pd) (mol/mol) = 5) was then added to form a dark-brown sol. After 30 min of sol generation, the colloid was immobilized by adding activated carbon (acidified at pH 1 by sulfuric acid) under vigorous stirring conditions. The amount of support material required was calculated so as to have a total final metal loading of 1 wt %. After 2 h, the slurry was filtered and the catalyst was washed thoroughly with distilled water (neutral mother liquors) and dried at 120 °C for 16 h.

Catalyst Characterization

- *Powder X-ray diffraction (p-XRD)*

Powder X-ray diffraction (p-XRD) patterns (Figure 1b) were acquired using a Bruker D8 ADVANCE A25-X1 powder diffractometer in Bragg Brentano geometry employing a Co K_α radiation source operating at 35kV and 40 mA ($\Delta 2\Theta$ =0.009°, count time= 112.32s/step). A LYNXEYE XE-T energy dispersive 1D detector was used. The reference diffraction peaks for Pd (111) (JCPDS no: 46-1043) and PdO (101) (JCPDS no: 41-1107) measured with Cu K_α were converted to Co K_α using the following relation: $2\Theta\,(\text{Co}) = 114.59156 \cdot \text{asin}(1.7891 / 1.5418 \cdot \sin(0.00872664 \cdot 2\Theta\,(\text{Cu})))$.

In-situ p-XRD (Figure 1c) was carried out using an X'pert Pro XRD fitted with an Anton-Parr XRK900 in-situ cell (internal volume of 0.5 L) with XRD patterns recorded between 30-80° 2θ employing a Cu K_α radiation source operating at 40 keV and 40 mA. A flow of Ar (15 ml min^{-1}) was passed through the sample bed whilst the cell was heated to 350 °C (5 °C min^{-1}) and was

kept for 5 min at a selected temperature before the diffraction patterns were collected. The spectra were analysed using X'Pert High Score Plus software.

- *X-ray Photoemission Spectroscopy (XPS)*

Fresh powder materials - X-ray Absorption Spectroscopy (XPS) was performed by using a Thermo Scientific K-alpha photoelectron spectrometer with monochromatic Al Kα radiation. The resulting spectra were processed in CasaXPS and calibrated against the C(1s) line at 284.7 eV.

Electrode materials - The surface composition of PdClx/C prior to and after electrochemical stability testing was determined on a Quantera II (Physical Electronics, Chanhassen, MN, USA), applying a monochromatic Al Kα X-ray source (1486.6 eV) operating at 15 kV and 25 W. The C1s signal was referenced to 284.8 eV.

- *X-ray Absorption Spectroscopy (XAS)*

X-ray absorption fine structure (XAFS) for all the Pd/C samples at the Pd K absorption edge, were recorded in transmission mode, at the B18 beamline of Diamond Light Source, Harwell, UK. The measurements were performed using a QEXAFS set-up with a fast-scanning Si (111) double crystal monochromator. The Demeter software packages (Athena and Artemis) were used for XAFS data analysis of the Pd/C absorption spectra in comparison to standards relative to a Pd foil. The XANES spectra at the Cl K-edge were recorded at the BM28 (XMaS) beamline at the European Synchrotron Radiation Facility (ESRF) in Grenoble (France). The spectra were acquired in fluorescence mode. The fluorescent signal was detected using a silicon drift diode detector. PyMca software, developed by the Software Group of the European Synchrotron Radiation Facility (ESRF), was used for the spectra analysis.

- *Electron Microscopy*

Scanning transmission electron microscopy measurements has been carried out on JEM-2200FS (Jeol) operating at 200 kV and on a FEI TITAN aberration-corrected (CEOS) electron microscope operating at 300 kV equipped with an HAADF detector (73-352 mrad).

Electrochemical Reactivity

A three compartment in-house prepared Teflon cell was used as electrochemical cell. The electrochemistry measurements were performed at room temperature (25 °C). As reference electrode, a saturated Ag/AgCl reference electrode (Metrohm) was used, a graphite rod was used as counter electrode. Both are placed in separate compartments of the electrochemical cell separated by a Nafion membrane. As a working electrode, a commercially available RRDE tip was used (AFE6R1PT, Pine Research Instrumentation), consisting of a glassy carbon disc

(0.196 cm^2) and a Pt ring (1 mm thickness) embedded in a Peek tip. A catalyst ink in ultra-pure water (18 MΩ, TOC < 3 ppb, ELGA) was prepared and dropcasted onto the glassy carbon electrode. An electrode loading of 10 μg_{metal} cm^{-2} was used for all RRDE measurements. As electrolyte, 0.1 M $HClO_4$, prepared from ultra-pure water and concentrated suprapure acid (Merck, Suprapur) was used. The collection efficiency (0.22) of the ring was determined experimentally by calibration of the 1-electron redox couple ferrocyanide($[Fe(CN)_6]^{4-}$)/ferricyanide($[Fe(CN)_6]^{3-}$) at different rotation rates. During RRDE measurements, the ring potential was set to a constant potential of 1.28 V_{RHE}. For the determination of Pd leaching during cycling, aliquots were taken after different times and analyzed via ICP-MS. ICP-MS analysis was performed on a NexION 300X from Perkin Elmer. The quantitative determination of ^{106}Pd content was obtained by comparison to calibrated internal standard solutions of ^{103}Rh. A four-point calibration was done before each measurement. For HOR measurement, a catalyst loading of 0.00198 mg_{Pd} cm^{-2} and the same Teflon cell as for RRDE measurements were used.

H_2O_2 Synthesis and Degradation - Hydrogen peroxide synthesis and degradation activity was evaluated using a Parr Instruments stainless steel autoclave with a nominal volume of 100 ml. To test each catalyst for H_2O_2 synthesis, the autoclave was charged with catalyst (0.01g) and 8.5 g solvent (5.6 g MeOH and 2.9 g H_2O both HPLC grade). The charged autoclave was then purged three times with 5% H_2/CO_2 (7 bar) before 5% H_2/CO_2 to a pressure of 29 bar followed by the addition of 25% O_2/CO_2 (11 bar). The temperature was then allowed to decrease to 2 °C followed by stirring (at 1200 rpm) of the reaction mixture for 30 mins. The H_2O_2 productivity was determined by titrating aliquots of the final solution after reaction with acidified $Ce(SO_4)_2$ (0.01 M) in the presence of two drops of ferroin indicator. H_2O_2 degradation experiments were carried out in a similar manner to the H_2O_2 synthesis experiments, but in the absence of 25%O_2/CO_2. Furthermore, H_2O from the 8.5 g of solvent was replaced by a 50 vol% H_2O_2 solution to give a reaction solvent containing between 4 wt% H_2O_2. The standard reaction conditions adopted for H_2O_2 degradation were as follows: 0.01 g catalyst, 8.5 g solvent (5.6 g MeOH, 2.22 g H_2O and 0.68 g H_2O_2 (50 %)), 29 bar 5%H_2/CO_2, 2 °C, 1200 rpm, 30 mins.

Figure 1 – Characterization of as prepared 1% $PdCl_x$/C catalyst by a) Pd $3d_{5/2}$ X-ray photoelectron spectroscopy b) X-ray diffraction. Bare carbon and Pd_{np}/C are shown for comparison. c) *in situ* X-ray diffraction at increasing temperatures under a flow of Ar d) Representative TEM images and e) HAADF-STEM images.

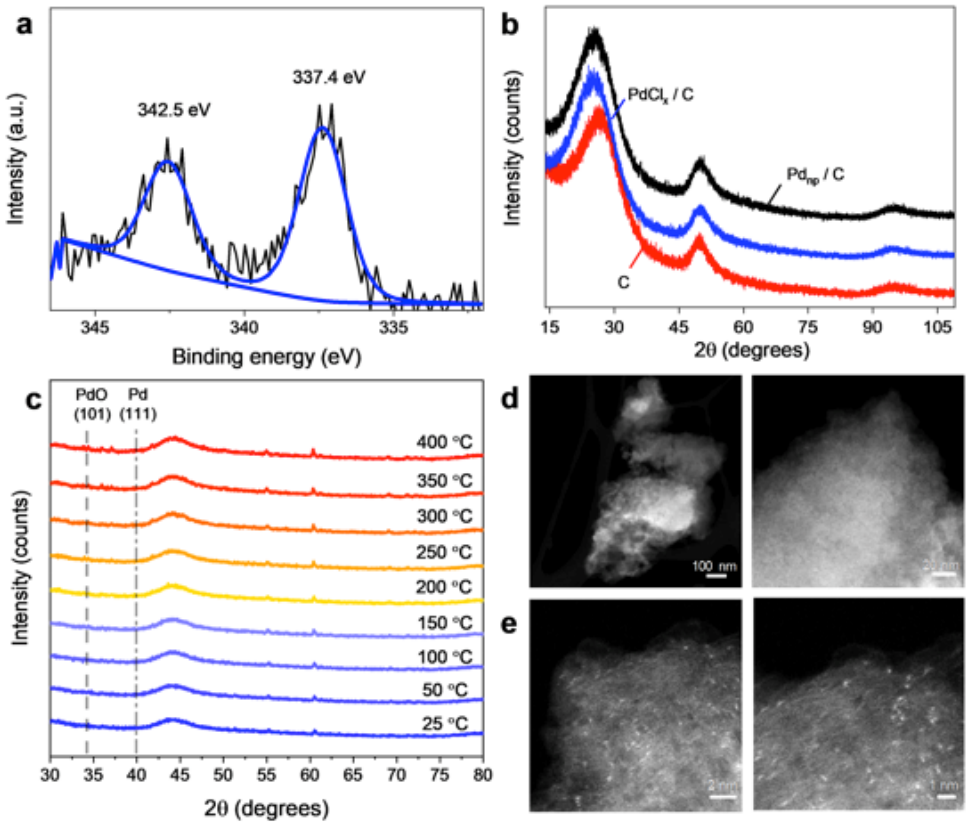

Figure 2 (a-d) – Pd K-edge X-ray absorption spectra and k^3 weighted Fourier transform (FT) magnitude of the as prepared $PdCl_x/C$ and Pd standards (Pd foil, PdO, $PdCl_2$) **e)** Cl K-edge X-ray absorption spectra of the fresh $PdCl_x/C$ catalyst material.

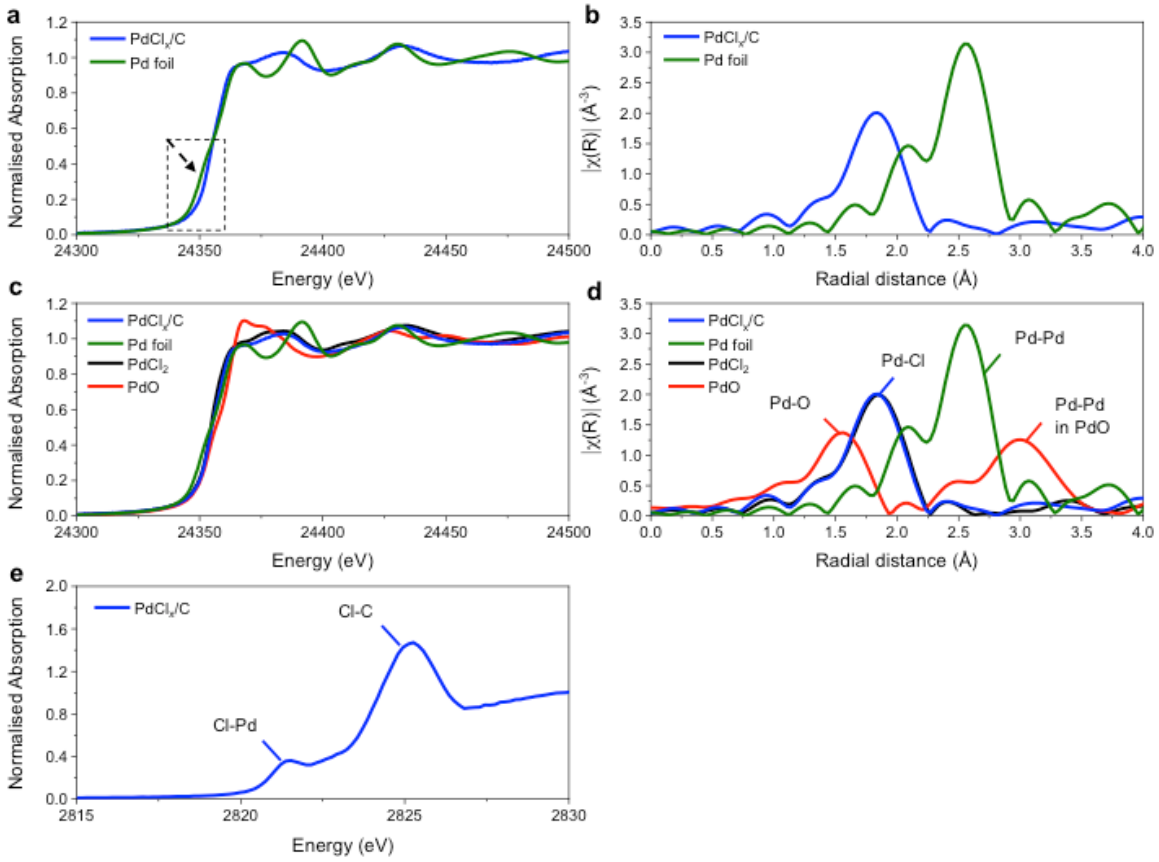

Figure 3 – a) Cyclic voltammogram at 50 mV s^{-1} between 0.1 and 1.6 V_{RHE} in Ar-saturated 0.1 M $HClO_4$ of $PdCl_x/C$ and Pd_{np}/C). **b)** Cyclic voltammetry of $PdCl_x/C$ at 50 mV s^{-1} at different rotation speeds (0, 400, 900, 1600, 2500 rpm) in hydrogen saturated $HClO_4$ between -0.005 V_{RHE} and 0.775 V_{RHE}. **c)** RRDE results for $PdCl_x/C$, Pd_{np}/C and C in O_2-saturated 0.1 M $HClO_4$ at 50 mV s^{-1} and 900 rpm, potential scan from 0.1 until 1.2 V and **d)** the corresponding potential depended selectivities $S_{H_2O_2}$.

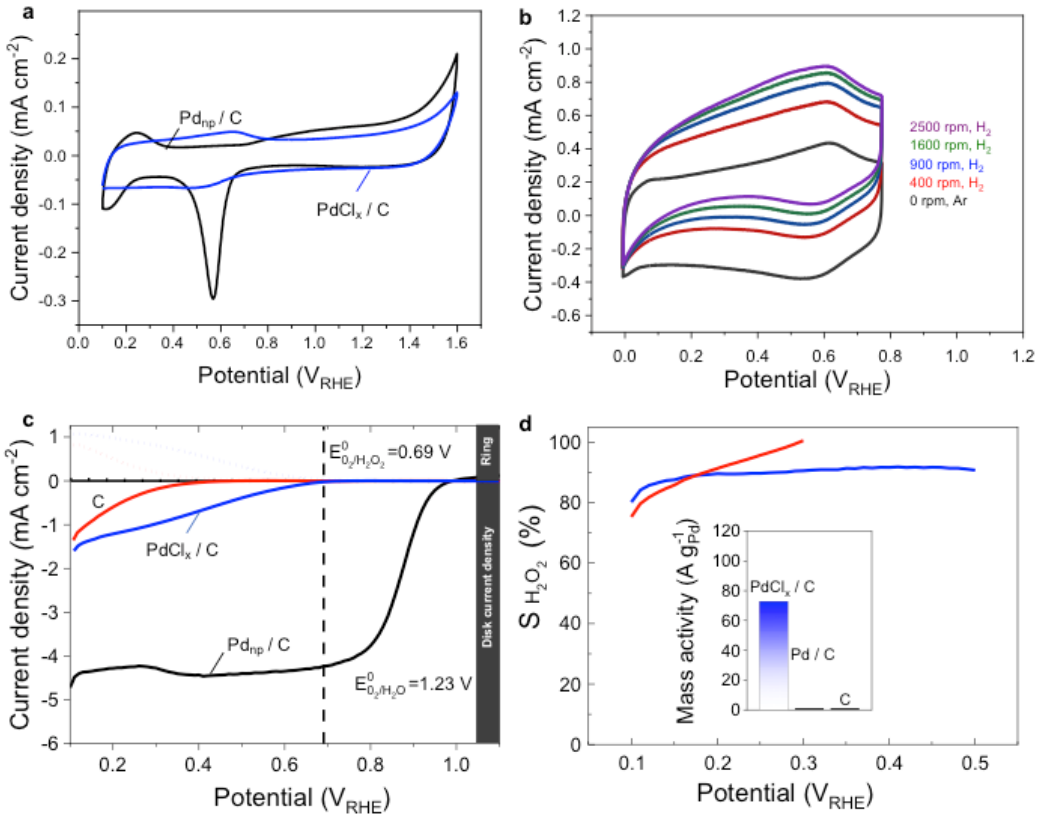

Figure 4 – a, b) Pd 3d and Cl 2p XPS characterization of fresh $PdCl_x/C$ (BOL) and after 1000 potential cycles between 0.05 and 0.8 V_{RHE} at 1 V s^{-1} (EOL)**. c, d)** Pd K-edge X-ray absorption spectra and k^3 weighted Fourier transform (FT) magnitude of the as prepared $PdCl_x/C$ before and after the direct H_2O_2 synthesis reaction. **e)** Pd mass loss in a three-compartment cell in $HClO_4$ monitored via ICP-MS after holding the working electrode at open circuit potential (OCP), after activity/selectivity measurements (c.f. figure 3) and after different numbers of degradation cycles between 0.05 and 0.8 V_{RHE} at 1 V s^{-1}

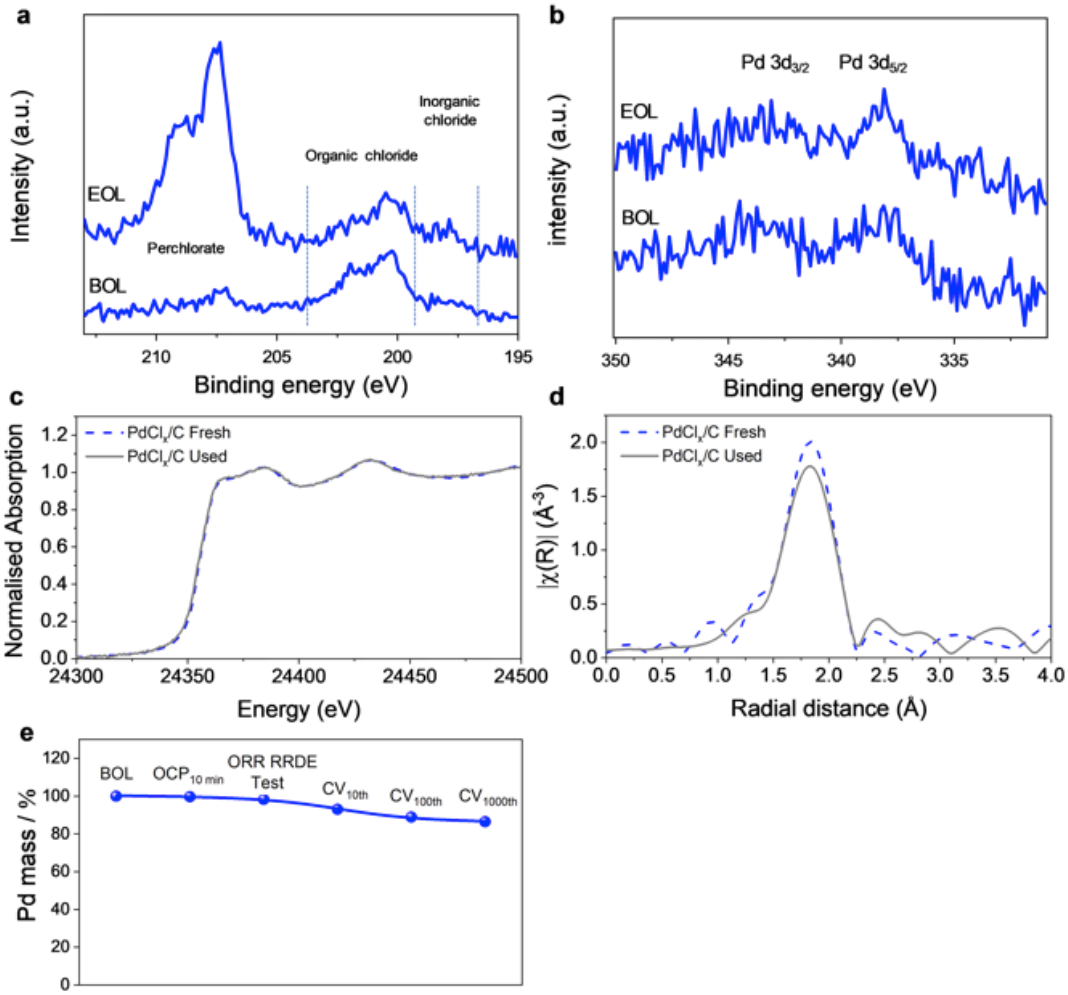

Supporting Information

Supporting information contains additional catalyst characterization (XPS and TEM), EXAFS fitting parameters, extended CV measurements and comparisons with the heterogeneous and electrocatalysis literature.

Acknowledgments

ML acknowledge the Federal Ministry of Education and Research (BMBF) in the framework of NanoMatFutur (SynKat, FK: 03XP0265) for financial support. KJJM acknowledges the Federal Ministry for Economic Affairs and Energy (BMWi) of Germany in the framework of PtTM@HGS (project number 03ET6080A). EP acknowledges financial support from the IMPRS-SurMat doctoral program. Andrea Mingers is thanked for help with the ICP-MS. We thank Alexander Auer and Corentin Poidevin for fruitful discussions. We thank the MAXNET Energy and Cardiff University for the financial support of the project. SF acknowledges the University of Bath for the award of a Prize Research Fellowship in Sustainable Technology. The authors thank the UK Catalysis Hub for allocating beamtime through the UK Catalysis Hub BAG allocation for X-ray acquisition of the absorption spectroscopic data at the Diamond synchrotron facility (SP15151).

References

1. Jones, C. W. Applications of Hydrogen Peroxide and Derivatives, The Royal Society of Chemistry, Cambridge **1999**, 207-230.
2. Russo, V.; Tesser, R.; Santacesaria E.; Di Serio. M. Chemical and Technical Aspects of Propene Oxide Production via Hydrogen Peroxide (HPPO Process), *Ind. Eng. Chem. Res.*, **2013**, *52*, 1168-1178.
3. Chen, Z.; Chen, S.; Siahrostami, S.; Chakthranont, P.; Hahn, C.; Nordlund, D.; Dimosthenis, S.; Nørskov, J. K.; Bao, Z.; Jaramillo, T. F. Development of a reactor with carbon catalysts for modular-scale, low-cost electrochemical generation of H_2O_2. *React. Chem. Eng.*, **2017**, *2*, 239-245.
4. Chen, Q. Development of an anthraquinone process for the production of hydrogen peroxide in a trickle bed reactor—From bench scale to industrial scale *Chem. Eng.Proc.*, **2008**, *47*, 787-792.
5. Campos-Martin, J. M.; Blanco-Brieva G.; Fierro, J. L. G. Hydrogen peroxide synthesis: an outlook beyond the anthraquinone process. *Angew. Chem. Int. Ed.*, **2006**, *45*, 6962-6984.

6. García-Serna, J.; Moreno, T.; Biasi, P.; Cocero, M. J.; Mikkola, J. P.; Salmi, T. O. Engineering in direct synthesis of hydrogen peroxide: targets, reactors and guidelines for operational conditions. *Green Chem.*, **2014**, *16*, 2320-2343.
7. Henkel H.; Weber, W. *US Patent 1,108,752,* **1914**.
8. Samanta, C. Direct synthesis of hydrogen peroxide from hydrogen and oxygen: An overview of recent developments in the process. *App. Catal. A: Gen.*, **2008**, *350*, 133-149.
9. Edwards, J. K.; Freakley, S. J.; Lewis, R. J.; Pritchard, J. C.; Hutchings, G. J. Advances in the direct synthesis of hydrogen peroxide from hydrogen and oxygen. *Catal Today*, **2015**, *248***,** 3-9.
10. Lewis, R. J.; Hutchings, G. J. Recent Advances in the Direct Synthesis of H_2O_2 *ChemCatChem*, **2019**, *11*, 298-308.
11. Seo, M. G.; Kim, H. J.; Han S. S.; Lee, K. Y. Direct Synthesis of Hydrogen Peroxide from Hydrogen and Oxygen Using Tailored Pd Nanocatalysts: A Review of Recent Findings. *Catal. Surv. Asia*, **2017**, *21*, 1-12.
12. Yi, Y.; Wang, L.; Li, G.; Guo, H. A review on research progress in the direct synthesis of hydrogen peroxide from hydrogen and oxygen: noble-metal catalytic method, fuel-cell method and plasma method. *Catal. Sci. Technol.*, **2016**, *6*, 1593-1610.
13. Menegazzo, F.; Signoretto, M.; Ghedini, E.; Strukul, G. Looking for the "Dream Catalyst" for Hydrogen Peroxide Production from Hydrogen and Oxygen *Catalysts*, **2019**, *9*, 251.
14. Ranganathan, S. S.; Sieber, V. Recent Advances in the Direct Synthesis of Hydrogen Peroxide Using Chemical Catalysis—A Review. *Catalysts*, **2018**, *8*, 379.
15. Choudhary, V. R.; Samanta C.; Jana, P. Decomposition and/or hydrogenation of hydrogen peroxide over Pd/Al_2O_3 catalyst in aqueous medium: Factors affecting the rate of H_2O_2 destruction in presence of hydrogen. *App. Catal. A: Gen.*, **2007**, *332*, 70-78.
16. Choudhary, V. R.; Ingole, Y. V.; Samanta C.; Jana, P. Direct oxidation of hydrogen to hydrogen peroxide over Pd (or PdO)/Al_2O_3 in aqueous reaction medium: influence of different acids and halide anions in reaction medium on formation and destruction of H_2O_2. *Ind. Eng. Chem. Res.*, **2007**, *46*, 8566-8573.
17. Centomo, P.; Meneghini, C.; Sterchele, S.; Trapananti, A.; Aquilanti G.; Zecca, M. EXAFS in situ: The effect of bromide on Pd during the catalytic direct synthesis of hydrogen peroxide. *Catal. Today*, **2015**, *248*, 138-141.
18. Edwards, J. K.; Freakley, S. J.; Carley, A. F.; Kiely C. J.; Hutchings G. J. Strategies for Designing Supported Gold–Palladium Bimetallic Catalysts for the Direct Synthesis of Hydrogen Peroxide. *Acc. Chem. Res.*, **2014**, *47*, 845-854.

19. Edwards, J. K.; Hutchings G. J. Palladium and gold-palladium catalysts for the direct synthesis of hydrogen peroxide. *Angew. Chem. Int. Ed.*, **2008**, *47*, 9192-9198.

20. Edwards, J. K.; Solsona, B.; Ntanjua, E. N.; Carley, A. F.; Herzing, A. A.; Kiely, C. J.; Hutchings, G. J. Switching off hydrogen peroxide hydrogenation in the direct synthesis process. *Science*, **2009**, *323*, 1037-1041.

21. Freakley, S. J.; He, Q.; Harrhy, J. H.; Lu, L.; Crole, D. A.; Morgan, D. J.; Ntainjua, E. N.; Edwards, J. K.; Carley, A. F.; Borisevich, A. Y.; Kiely, C. J.; Hutchings, G. J. Palladium-tin catalysts for the direct synthesis of H_2O_2 with high selectivity. *Science*, **2016**, *351*, 965-968.

22. Maity, S.; Eswaramoorthy, M. Ni–Pd bimetallic catalysts for the direct synthesis of H_2O_2 – unusual enhancement of Pd activity in the presence of Ni. *J. Mater. Chem. A*, **2016**, *4*, 3233-3237.

23. Wang, S.; Gao, K.; Li, W.; Zhang, J. Effect of Zn addition on the direct synthesis of hydrogen peroxide over supported palladium catalysts**.** *App. Catal. A: Gen.*, **2017**, *531*, 89-95.

24. Wilson, N. M.; Schröder, J.; Priyadarshini, P.; Bregante, D. T.; Kunz, S.; Flaherty D. W. Direct synthesis of H_2O_2 on PdZn nanoparticles: The impact of electronic modifications and heterogeneity of active sites. *J. Catal.*, **2018**, *368*, 261-274.

25. Wilson, N. M.; Flaherty, D. W. Mechanism for the Direct Synthesis of H_2O_2 on Pd Clusters: Heterolytic Reaction Pathways at the Liquid–Solid Interface. *J.A.C.S.*, **2016**, *138*, 574-586.

26. Yang, S.; Verdaguer Casadevall, A.; Arnarson, L.; Silvioli, L.; Čolić, V.; Frydendal, R.; Rossmeisl, J.; Chorkendorff, I.; Stephens, I. E. L. Toward the Decentralized Electrochemical Production of H_2O_2: A Focus on the Catalysis. *ACS Catal.*, **2018**, *8*, 4064-4081.

27. Jiang, Y.; Ni, P.; Chen, C.; Lu, Y.; Yang, P.; Kong, B.; Fisher, A.; Wang, X. Selective Electrochemical H_2O_2 Production through Two Electron Oxygen Electrochemistry. *Adv. Energy Mater.*, **2018**, *8*, 1801909.

28. Fortunato, G.V.; Pizzutilo, E.; Mingers, A. M.; Kasian, O.; Cherevko, S.; Cardoso, E. S. F.; Mayrhofer, K. J. J.; Maia, G.; Ledendecker, M. Impact of Palladium Loading and Interparticle Distance on the Selectivity for the Oxygen Reduction Reaction toward Hydrogen Peroxide. *J. Phys. Chem. C,* **2018**, *122 (28)*, 15878-15885.

29. Wang, Y. L.; Gurses, S.; Felvey, N.; Boubnov, A.; Mao, S. S.; Kronawitter, C. X. In Situ Deposition of Pd during Oxygen Reduction Yields Highly Selective and Active Electrocatalysts for Direct H_2O_2 Production. *ACS Catalysis* **2019,** *9* (9), 8453-8463.

30. Colic, V.; Yang, S.; Revay, Z.; Stephens, I. E. L; Chorkendorff, I. Carbon catalysts for electrochemical hydrogen peroxide production in acidic media. *Electrochem. Acta* **2018**, 272, 192-202.

31. Katsounaros, I.; Schneider, W. B.; Meier, J. C.; Benedikt, U.; Biedermann, P. U.; Cuesta, A.; Auer, A. A.; Mayrhofer, K. J. J. The impact of spectator species on the interaction of H_2O_2 with platinum – implications for the oxygen reduction reaction pathways**.** *Phys. Chem. Chem. Phys.*, **2013**, *15*, 8058-8068.

32. Choi, C. H.; Kwon, H. C.; Yook, S.; Shin, H.; Kim, H.; Choi, M. Hydrogen Peroxide Synthesis via Enhanced Two-Electron Oxygen Reduction Pathway on Carbon-Coated Pt Surface. *J. Phys. Chem. C*, **2014**, **118**, 30063-30070.

33. Pizzutilo, E.; Freakley, S. J.; Cherevko, S.; Venkatesan, S.; Hutchings, G. J.; Liebscher, C. H.; Dehm, G.; Mayrhofer, K. J. J. Gold–Palladium Bimetallic Catalyst Stability: Consequences for Hydrogen Peroxide Selectivity. *ACS Catal.*, **2017**, *7*, 5699-5705.

34. Chen, D.; Li, J.; Cui, P.; Liu, H.; Yang, J. Gold-catalyzed formation of core–shell gold–palladium nanoparticles with palladium shells up to three atomic layers. *J. Mater. Chem. A*, **2016**, *4*, 3813-3821.

35. Pizzutilo, E.; Kasian, O.; Choi, C. H.; Cherevko, S.; Hutchings, G. J.; Mayrhofer, K. J. J.; Freakley, S. J. Electrocatalytic synthesis of hydrogen peroxide on Au-Pd nanoparticles: From fundamentals to continuous production. *Chem. Phys Lett.*, **2017**, *683*, 436-442.

36. Siahrostami, S.; Verdaguer-Casadevall, A.; Karamad, M.; Deiana, D.; Malacrida, P.; Wickman, B.; Escudero-Escribano, M.; Paoli, E. A.; Frydendal, R.; Hansen, T. W.; Chorkendorff, I.; Stephens, I. E. L.; Rossmeisl, J. Enabling direct H_2O_2 production through rational electrocatalyst design. *Nat. Mater.*, **2013**, *12*, 1137-1143.

37. Verdaguer-Casadevall, A.; Deiana, D.; Karamad, M.; Siahrostami, S.; Malacrida, P.; Hansen, T. W.; Rossmeisl, J.; Chorkendorff, I.; Stephens, I. E. L. Trends in the electrochemical synthesis of H_2O_2: enhancing activity and selectivity by electrocatalytic site engineering. *Nano Lett.*, **2014**, *14*, 1603-1608.

38. Yang, S.; Tak, Y. J.; Kim, J.; Soon, A.; Lee, H. Support Effects in Single-Atom Platinum Catalysts for Electrochemical Oxygen Reduction. *ACS Catal.*, **2017**, *7*, 1301-1307.

39. Yang, S.; Kim, J.; Tak, Y. J.; Soon, A.; Lee, H. Single-Atom Catalyst of Platinum Supported on Titanium Nitride for Selective Electrochemical Reactions. *Angew. Chem. Int. Ed.*, **2016**, *55*, 2058-2062.

40. Choi, C. H.; Kim, M.; Kwon, H. C.; Cho, S. J.; Yun, S.; Kim, H. T.; Mayrhofer, K. J. J.; Kim, H.; Choi, M. Tuning selectivity of electrochemical reactions by atomically dispersed platinum catalyst. *Nat. Commun.*, **2016**, *7,* 10922.

41. Yamanaka, I.; Ichihashi, R.; Iwasaki, T.; Nishimura, N.; Murayama, T.; Ueda, W.; Takenaka, S. *Electrochem. Acta,* **2013,** *108*, 321-329.

42. Jirkovský, J. S.; Ahlberg, E.; Panas I.; Schiffrin, D. J. The bifurcation point of the oxygen reduction reaction on Au–Pd nanoalloys. *Faraday Discuss.*, **2016**, *188*, 257-278.

43. Jirkovský, J. S.; Panas, I.; Romani, S.; Ahlberg, E.; Schiffrin, D. J. Potential-Dependent Structural Memory Effects in Au–Pd Nanoalloys. *J. Phys. Chem. Lett.*, **2012**, *3*, 315-321.

44. Malta, G.; Kondrat, S. A.; Freakley, S. J.; Davies, C. J.; Lu, L.; Dawson, S.; Thetford, A.; Gibson, E. K.; Morgan, D. J.; Jones, W.; Wells, P. P.; Johnston, P.; Catlow, C. R. A.; Kiely, C. J.; Hutchings, G. J. Identification of single-site gold catalysis in acetylene hydrochlorination. *Science*, **2017**, *355*, 1399-1403.

45. Noack, K.; Zbinden, H.; Schlögl, R. Identification of the state of palladium in various hydrogenation catalysts by XPS. *Catal. Lett.*, **1990**, *4*, 145-155.

46. Fujikawa, T.; Tsuji, K.; Mizuguchi, H.; Godo, H.; Iedi, K.; Usui, K. EXAFS characterization of bimetallic Pt–Pd/SiO_2–Al_2O_3 catalysts for hydrogenation of aromatics in diesel fuel *Catal. Lett.*, **1999**, *63*, 27-33.

47. Leri, A. C.; Marcus, M. A.; Myneni, S. C. B. Quantitative speciation of absolute organohalogen concentrations in environmental samples by X-ray absorption spectroscopy. *Geochim. Cosmochim. Acta,* **2007**, *71*, 5834-5846.

48. Lopes, C. W.; Cerrillo, J. L.; Palomares, A. E.; Rey, F.; Agostini, G. An *in situ* XAS study of the activation of precursor-dependent Pd nanoparticles *Phys. Chem. Chem. Phys.*, **2018**, *20*, 12700-12709.

49. Liu, Y.; Zhou, Y.; Li, J.; Wang, Q.; Qin, Q.; Zhang, W.; Asakura, H.; Yan. N.; Wang, J. Direct aerobic oxidative homocoupling of benzene to biphenyl over functional porous organic polymer supported atomically dispersed palladium catalyst. *Appl. Catal. B: Environ.* **2017**, 205, 679-688.

50. Pizzutilo, E.; Freakley, S. J.; Geiger, S.; Baldizzone, C.; Mingers, A.; Hutchings, G. J.; Mayrhofer, K. J. J.; Cherevko, S. Addressing stability challenges of using bimetallic electrocatalysts: the case of gold–palladium nanoalloys *Catal. Sci. Technol.*, **2017**, *7*, 1848-1856.

51. Pritchard, J.; Kesavan, L.; Piccinini, M.; He, Q.; Tiruvalam, R.; Dimitratos, N.; Lopez-Sanchez, J. A.; Carley, A. F.; Edwards, J. K.; Kiely, C. J.; Hutchings, G. J. Direct

Synthesis of Hydrogen Peroxide and Benzyl Alcohol Oxidation Using Au−Pd Catalysts Prepared by Sol Immobilization. *Langmuir*, **2010**, *26*, 16568-16577.

52. Tian, P.; Ouyang, L.; Xu, X.; Ao, C.; Xu, X.; Si, R.; Shen X.; Lin, M.; Xu, J.; Han, Y. F. The origin of palladium particle size effects in the direct synthesis of H_2O_2: Is smaller better? *J. Catal.*, **2017**, *349*, 30-40.
53. Vilé, G.; Albani, D.; Nachtegaal, M.; Chen, Z.; Dontsova, D.; Antonietti, M.; López N.; Pérez-Ramírez, J. A stable single-site palladium catalyst for hydrogenations. *Angew. Chem. Int. Ed.,* **2015**, *54*, 11265-11269.
54. Łosiewicz, B.; Birry, L.; Lasia, A. Effect of adsorbed carbon monoxide on the kinetics of hydrogen electrosorption into palladium. *J. Electroanal. Chem.*, **2007**, *611*, 26-34.
55. Selinsek, M.; Deschner, B. J.; Doronkin, D. E.; Sheppard, T. L.; Grunwaldt J. D.; Dittmeyer, R. Revealing the Structure and Mechanism of Palladium during Direct Synthesis of Hydrogen Peroxide in Continuous Flow Using Operando Spectroscopy. *ACS Catal.*, **2018**, *8*, 2546-2557.
56. Kanungo, S.; van Haandel, L.; Hensen, E. J. M.; Schouten J. C.; Neira d'Angelo, M. F.; Direct synthesis of hydrogen peroxide in AuPd coated micro channels: an in-situ XAS study**.** *J. Catal.*, **2019**, *370*, 200-209.
57. Mayrhofer, K. J. J.; Strmcnik, D.; Blizanac, B. B.; Stamenkovic, V.; Arenz M.; Markovic, N. M. Measurement of oxygen reduction activities via the rotating disc electrode method: From Pt model surfaces to carbon-supported high surface area catalysts. *Electrochim. Acta*, **2008**, *53*, 3181-3188.
58. Strmcnik, D.; Uchimura, M.; Wang, C.; Subbaraman, R.; Danilovic, N.; van der Vliet, D.; Paulikas, A. P.; Stamenkovic V. R.; Markovic, N. M. Improving the hydrogen oxidation reaction rate by promotion of hydroxyl adsorption. *Nat. Chem.*, **2013**, *5*, 300-306.
59. Wilson, N. M.; Priyadarshini, P.; Kunz S.; Flaherty, D. W. Direct synthesis of H_2O_2 on Pd and Au_xPd_1 clusters: Understanding the effects of alloying Pd with Au. *J. Catal.*, **2018**, *357*, 163-175.